Quantum Electronics **45** (10) 879 – 883 (2015) ©2015 Kvantovaya Elektronika and Turpion Ltd

LASERS

PACS numbers: 42.55.Px; 42.60.Da; 42.60.Jf
DOI: 10.1070/QE2015v045n10ABEH015844

Optimisation of cavity parameters for lasers based on AlGaInAsP/InP solid solutions (λ = 1470 nm)

D.A. Veselov, K.R. Ayusheva, I.S. Shashkin, K.V. Bakhvalov, V.V. Vasil'eva, L.S. Vavilova, A.V. Lyutetskiy, N.A. Pikhtin, S.O. Slipchenko, Z.N. Sokolova, I.S. Tarasov

Abstract. **We have studied the effect of laser cavity parameters on the light – current characteristics of lasers based on the AlGaInAs/GaInAsP/InP solid solution system that emit in the spectral range 1400 – 1600 nm. It has been shown that optimisation of cavity parameters (chip length and front facet reflectivity) allows one to improve heat removal from the laser, without changing other laser characteristics. An increase in the maximum output optical power of the laser by 0.5 W has been demonstrated due to cavity design optimisation.**

Keywords: *semiconductor laser, saturation of the light – current characteristic, Auger recombination, laser cavity.*

1. Introduction

High-power semiconductor lasers operating in the range 1400 – 1600 nm are of considerable interest for practical application. The low loss in optical fibres at a wavelength of 1550 nm and the fact that laser light in this spectral range is comparatively safe to the human eye make such devices indispensable in resolving a variety of issues. Lasers based on the AlGaInAs/GaInAsP/InP solid solution system have already demonstrated the possibility of operation with considerable output power [1 – 8].

Nevertheless, the development of laser nanoheterostructures and lasers based on this material system that emit in the above spectral range is a challenging problem because a number of effects, such as Auger recombination and carrier escape from the active region, reduce the laser efficiency by virtue of specific features of the solid solution system and should be taken into account in designing instruments.

In this paper, we examine the effect of cavity parameters on the power performance of semiconductor lasers based on the AlGaInAs/GaInAsP/InP solid solution system. Our main purpose here is to optimise the cavity parameters for raising the maximum laser output power.

D.A. Veselov, K.R. Ayusheva, I.S. Shashkin, K.V. Bakhvalov, V.V. Vasil'eva, L.S. Vavilova, A.V. Lyutetskiy, N.A. Pikhtin, S.O. Slipchenko, Z.N. Sokolova, I.S. Tarasov Ioffe Institute, Russian Academy of Sciences, Politekhnicheskaya ul. 26, 194021 St. Petersburg, Russia;
e-mail: nike@hpld.ioffe.ru, shashkin@mail.ioffe.ru

Received 24 April 2015; revision received 17 June 2015
Kvantovaya Elektronika **45** (10) 879 – 883 (2015)
Translated by O.M. Tsarev

2. Experimental samples

For our studies, we fabricated a separate-confinement double laser heterostructure with a quantum-confined active region comprising three 50-Å-thick InGaAs quantum wells (QWs) and a narrow AlGaInAs waveguide. The parameters of the structure are indicated in Table 1. The composition of the active region was chosen so as to reach a large optical confinement factor in the active region, thereby reducing the threshold carrier concentration and, as a consequence, suppressing Auger recombination in the QWs. The QW thickness was such that a single quantisation level was present in the conduction band.

Table 1. Parameters of the laser heterostructure.

Layer	Thick-ness/μm	Material	Absorption edge wave-length/μm	Dopant type and concentra-tion/cm^{-3}
Substrate	350	InP	–	n, 3×10^{18}
Buffer	0.15	InP	–	n, 3×10^{18}
Waveguide	0.57	AlGaInAs	1.1	
Quantum well	0.005	InGaAs	1.47	
Barrier	0.01	AlGaInAs	1.1	
Quantum well	0.005	InGaAs	1.47	Undoped
Barrier	0.01	AlGaInAs	1.1	
Quantum well	0.005	InGaAs	1.47	
Waveguide	0.28	AlGaInAs	1.1	
p-Emitter	1.1	InP	–	p, 4×10^{17}
Contact	0.23	GaInAsP	1.45	p, 6×10^{18}

The emitters and waveguide were made from AlGaInAs because this material allows thermal carrier escape from the active region to the waveguide to be suppressed. This is due to the fact that a typical magnitude of electron confinement in a QW (ΔE_c) that ensures lasing in the spectral range 1300 – 1800 nm in AlGaInAs/InP-based heterostructures is approximately twice that in the InGaAsP/InP system [9, 10]. The waveguide thickness and geometry chosen ensured fundamental transverse mode lasing.

Semiconductor lasers were fabricated using a standard shallow mesa etching process, with a stripe contact width of 100 μm. The active-element design chosen minimised the thermal resistance of the lasers. The lasers were investigated using relatively low pump current amplitudes (under 10 A), at which carrier spreading had no effect on their characteristics.

The lasers differed in cavity length and end facet reflectivities.

3. Analysis of laser operation modes at different cavity parameters

Lasers based on the AlInGaAs/GaInAsP/InP solid solution system, which emit in the spectral range 1400–1600 nm, are known to have higher internal optical losses in comparison with AlInGaAs/GaAs shorter wavelength lasers. The internal optical loss and the internal quantum efficiency of stimulated emission at the lasing threshold were determined using standard light–current (L–I) measurements on lasers differing in cavity length, with naturally cleaved end facets as mirrors, and were found to be 5.7 cm^{-1} and 93%, respectively. In addition, we determined the threshold current density as a function of total optical loss for the same samples.

To maintain high external differential quantum efficiency of a laser at a high level of internal optical losses, one should increase the useful loss, e.g. by reducing the length of the laser chip. This technological solution is, however, nonoptimal because it leads to an increase in current density in the sample, impairs heat dissipation and lowers the thermal stability of the laser threshold current. Moreover, increasing the total loss in the laser leads to an increase in threshold carrier concentration and, hence, in Auger recombination rate in the active region.

Another possible way of increasing the useful loss in the cavity is by using a highly antireflective output mirror. As shown earlier [11], reducing the reflectivity of both facets of a pulsed laser to 5% allows the linearity of its L–I characteristic to be improved.

With the advent of the possibility of utilising high-quality AlN coatings that ensure very low reflectivity (down to 0.2%) [12], the laser cavity length can be increased without reducing the external optical loss and, hence, the external differential quantum efficiency.

In the simplest case, the cavity parameters of a laser emitting in the spectral range 1400–1600 nm and having a highly antireflective output mirror can be optimised as follows. As shown by L–I measurements on samples differing in length and having naturally cleaved end facets as mirrors, the highest maximum output power and, accordingly, the lowest saturation of the L–I characteristic are offered by the lasers with a cavity length of 2 and 2.5 mm. The lasers with a longer cavity have a lower external quantum yield of stimulated emission, and the lasers with a shorter cavity show strong saturation of their L–I characteristic, due to the high carrier concentration in their active region and, hence, to fast Auger recombination. When a low-reflectivity end facet is used, it is reasonable to increase the cavity length in order to maintain the same external optical loss as in the lasers 2–2.5 mm long. This will allow the threshold carrier concentration not to be increased and the external differential quantum efficiency not to be reduced.

The external optical loss $\alpha_{\rm m}$ can be evaluated by the well-known formula

$$\alpha_{\rm m} = \frac{1}{2L}\ln\left(\frac{1}{R_1 R_2}\right), \tag{1}$$

where L is the length of the laser cavity, and R_1 and R_2 are the front (output) and rear facet reflectivities, respectively. According to (1), the average external optical loss in the lasers with a cavity length from 2 to 2.5 mm and naturally cleaved end facets as mirrors is 5.5 cm^{-1}. This value will be thought of as optimal for the heterostructure under consideration, with its inherent internal optical loss, Auger recombination and carrier delocalisation from the active region.

Figure 1 shows the external optical loss as a function of front facet reflectivity at different laser cavity lengths. The use of a low-reflectivity output facet allows the laser cavity length to be increased without increasing the external optical loss. An antireflective coating with reflectivity under 0.5% allows the laser cavity length to be increased to 5 mm, which will ensure a twofold increase in chip cooling efficiency.

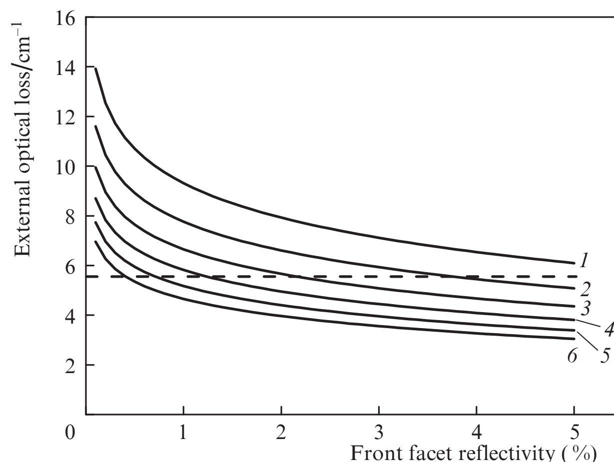

Figure 1. External optical loss as a function of front facet reflectivity for lasers with a cavity length of (*1*) 2.5, (*2*) 3, (*3*) 3.5, (*4*) 4, (*5*) 4.5 and (*6*) 5 mm. The dashed line represents the experimentally determined optimal external optical loss (5.5 cm^{-1}); λ = 1.47 μm.

Unfortunately, because of the nonuniform photon density and carrier concentration distributions along the cavity axis in the case of the low reflectivity of the laser output facet, the carrier concentration profile is severely distorted. Near the high-reflectivity facet, the carrier concentration increases, accelerating the Auger recombination process and leading to carrier escape from the active region, especially at elevated laser temperatures.

To determine the carrier concentration distribution along the cavity axis, we took advantage of the rate equations used previously for AlGaAs/GaAs/InGaAs lasers [11]. In this study, the model was modified to adjust it to AlGaInAs/GaInAsP/InP lasers. To take into account Auger recombination, the term $R_{\rm A}(n^{\rm QW})^3$ was included in the carrier balance equation:

$$\frac{{\rm d}n^{\rm QW}(z)}{{\rm d}t} = \frac{\eta J}{ed^{\rm QW}} - B(n^{\rm QW})^2 - \frac{c}{\sqrt{\varepsilon}}\frac{g(z)}{\Gamma}[S^+(z) + S^-(z)] - R_{\rm A}(n^{\rm QW})^3, \tag{2}$$

where $n^{\rm QW}$ is the three-dimensional carrier concentration in the quantum wells (the carrier concentration is thought to be the same in the three QWs); z is a coordinate along the longitudinal cavity axis; t is time; η is the fraction of charge carriers that reach the active region; J is the pump current density; e is the electron charge; $d^{\rm QW}$ is the total thickness of the QWs in the active region; B is the radiative recombination coefficient;

R_A is the Auger recombination coefficient; c is the speed of light in vacuum; ε is the relative dielectric permittivity of the waveguide in the laser; $g(z)$ is the coordinate-dependent modal gain coefficient; Γ is the optical confinement factor for radiation in the active region; and $S^+(z)$ and $S^-(z)$ are the photon densities in the counterpropagating flows. The total photon density at any point in the cavity is the sum of these two densities.

The dependence of the modal gain on the carrier concentration in the active region was taken into account as previously [11] and was corrected using experimental data on the threshold current density as a function of laser cavity length.

The radiative recombination coefficient B_{2D} for the QWs in the heterostructure under consideration was evaluated as [13]

$$B_{2D} = \frac{4}{3}\pi\alpha\sqrt{\varepsilon}\frac{\hbar}{(m_c + m_{hh})k_B T}E_0\left(\frac{P}{\hbar c}\right)^2, \tag{3}$$

where E_0 is the band gap energy corrected for size quantisation; $\alpha = e^2/(\hbar c)$ is the fine-structure constant; $\hbar$ is the Planck constant; k_B is the Boltzmann constant; T is the temperature in the active region; m_c is the conduction band electron mass; m_{hh} is the heavy hole mass in the valence band;

$$P^2 = \frac{\hbar}{2}\left(\frac{1}{m_c} - \frac{1}{m_{hh}}\right)\frac{E_g(E_g + \Delta)}{E_g + 2\Delta/3} \tag{4}$$

is the Kane parameter, determined using a formula from Ref. [13]; Δ is the spin–orbit splitting energy; and E_g is the band gap energy of the QWs.

The Auger recombination process was examined in a 3D layer approximation. The dominant mechanism in $Ga_xIn_{1-x}As$ solid solutions is Auger recombination involving the spin–orbit split-off valence band (CHHS process) [14]. According to Gel'mont et al. [15], the Auger recombination coefficient for the CHHS process is given by

$$R_A = \frac{18\pi e^4 m_c \hbar^3 (E_g + \Delta)^2}{\varepsilon^2 m_{hh} m_{SO}^2 E_g^5} I(\beta), \tag{5}$$

where

$$\beta = \frac{2m_{SO}}{m_{hh}}\frac{E_g - \Delta}{T}\frac{E_g^2}{(E_g + \Delta)(3E_g - 2\Delta)}; \tag{6}$$

m_{SO} is the hole effective mass in the spin–orbit split-off band; and the function $I(\beta)$ is represented in Fig. 2.

For $\beta \geqslant 10$, (5) transforms into the asymptotic expression

$$R_A = \frac{216\sqrt{2}\pi^{5/2}\hbar^3 e^4 m_c (E_g + \Delta)^2}{\varepsilon^2 m_{hh} m_{SO}^2 E_g^5 \sqrt{\beta}}\exp\left(-\frac{\beta}{2}\right). \tag{7}$$

Calculation of temperature-dependent R_A with consideration for the temperature variation of parameters of the InGaAs quantum well material indicates that the Auger recombination coefficient of this solid solution is a weak function of temperature, so its temperature variation can be left out of account.

The main purpose of the calculation was to optimise the laser cavity design with consideration for the nonuniform carrier concentration distribution. To avoid the necessity of taking into account the effect of temperature on laser processes, and in order not to include the heat equation in the starting system, the calculation was performed for pump currents no higher than three times the threshold value. At such pump currents, the $L-I$ characteristic of lasers having both of their end facets naturally cleaved did not deviate from linearity. The Auger recombination and radiative recombination coefficients, as well as carrier escape from the active region, can then be considered temperature-independent.

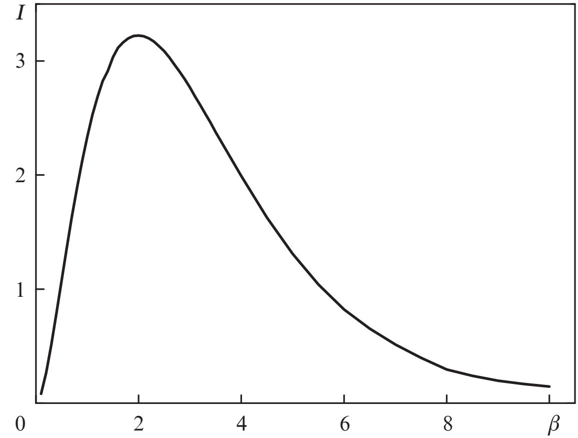

Figure 2. $I(\beta)$ curve for calculation of the Auger recombination coefficient for the process involving the spin–orbit split-off band.

The $L-I$ characteristic was calculated for lasers differing in cavity parameters. The rear facet reflectivity was taken to be 95% in all cases. The front facet reflectivity for a cavity of particular length was determined using Fig. 1. The calculation results are presented in Fig. 3.

It is seen in Fig. 3a that, at low pump currents, all of the $L-I$ curves are almost parallel, as would be expected in the case of roughly equal external optical losses. With increasing pump current, however, the curves diverge: at low front facet reflectivity ($R_1 < 1\%$) [curves (*5*), (*6*)], the $L-I$ characteristic of the laser saturates, even though the model does not take into account the increase in the temperature of the active region or in the internal optical loss with pump current. At the same time, the $L-I$ characteristics of the lasers with $R_1 >$ 1% [curves (*1*)–(*3*)] show no significant saturation.

It follows from the present results that, as the nonuniformity of the carrier concentration distribution along the cavity axis increases, the Auger recombination process in the region of the maximum concentration is so active that even a slight change in carrier concentration with increasing pump current leads to a considerable increase in Auger recombination rate and, as a consequence, to saturation of the $L-I$ characteristic.

Figure 3b shows the output optical power as a function of pump current density. The pump current density determines the temperature of the active region, the Auger recombination coefficient and carrier escape. It is for this reason that we endeavour to obtain high output optical power at low current density by increasing the cavity length. It is, however, seen from Fig. 3b that a proportional increase in cavity length and decrease in front facet reflectivity do not lead to a proportional increase in output optical power at a given current density. By contrast, because of the saturation, a decrease in front facet reflectivity and increase in cavity length lead to a progressively smaller increase in power.

Thus, the nonuniform carrier concentration distribution in the cavity of a semiconductor laser reduces the positive effect of an increase in cavity length and decrease in front facet reflectivity.

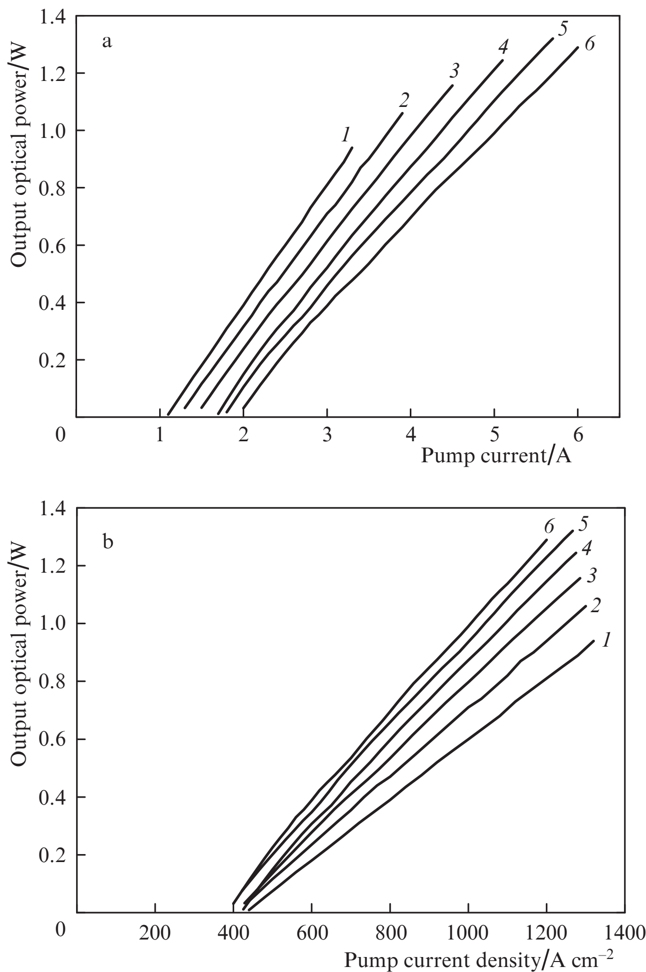

Figure 3. Calculated output power as a function of (a) pump current and (b) pump current density for lasers with the following cavity parameters: (*1*) L = 2.5 mm, R_1 = 5%; (*2*) 3 mm, 3.5%; (*3*) 3.5 mm, 2%; (*4*) 4 mm, 1%; (*5*) 4.5 mm, 0.75%; (*6*) 5 mm, 0.5%; λ = 1.47 µm.

4. Experimental study of the laser with the optimal cavity design

Analysis of Fig. 3 led us to choose the following cavity parameters: L = 4 mm and R_1 = 1% [curves (*4*)]. According to calculations, the length of such a cavity provides certain advantages in terms of heat dissipation, without saturation of its $L-I$ characteristic.

For comparison, we fabricated lasers with L = 2620 µm, R_1 = 5% and R_2 = 95% and ones with L = 3900 µm, R_1 = 1% and R_2 = 95%. Their power characteristics were measured in continuous mode. Figure 4 shows their experimentally determined $L-I$ curves. It is seen that, by optimising cavity parameters (a longer cavity length and lower front facet reflectivity), we were able to raise the maximum output optical power by 0.5 W due to better thermal conditions of laser operation.

5. Conclusions

It has been shown that optimisation of cavity parameters makes it possible to increase the pump current of a semiconductor laser emitting in the spectral range 1400–1600 nm, without changing other laser characteristics. This allows one to raise the maximum output optical power of the laser, with no saturation of its light–current characteristic.

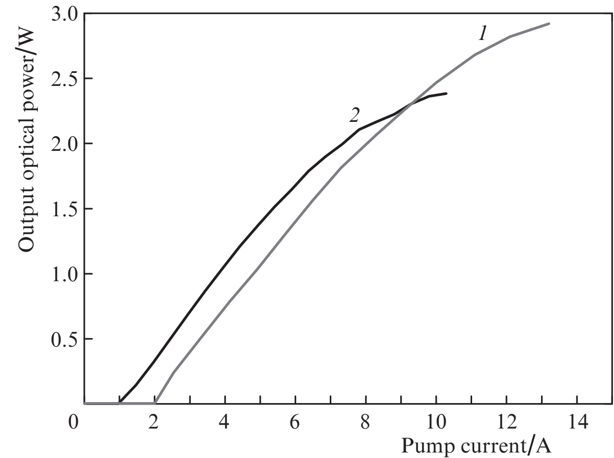

Figure 4. Experimentally determined light–current curves of cw lasers with the following cavity parameters: (*1*) L = 3900 µm, R_1 = 1%, R_2 = 95%; (*2*) 2620 µm, 5%, 95%; λ = 1.47 µm.

The possible increase in chip length and decrease in front facet reflectivity are limited by the formation of a nonuniform carrier distribution in the active region of the laser, which increases the Auger recombination rate, promotes carrier escape from the active region and leads to additional saturation of the $L-I$ characteristic. For lasers based on the heterostructure studied, the optimal front facet reflectivity is near 1% at a cavity length of ~4 mm. This optimisation of the cavity parameters allowed the maximum output optical power of the laser operating in continuous mode to be increased by 0.5 W.

Acknowledgements. This work was supported by the RF Ministry of Education and Science through the federal targeted programme 'Research and Development in the Priority Areas of the Science and Technology Sector of Russia in 2014–2020' and the applied research programme 'Development of the MOCVD Process with Application to Nanoheterostructures and Related High-Power CW and Pulsed Semiconductor Lasers Emitting in the Wavelength Range 1400–1600 nm' (No. 2014-14-579-0066-003, Agreement No. 14.607.21.0048, unique applied research identifier RFMEFI60714X0048).

References

1. Golikova E.G., Kureshov V.A., Leshko A.Yu., Livshits D.A., Lyutetskiy A.V., Nikolaev D.N., Pikhtin N.A., Ryaboshtan Yu.A., Slipchenko S.O., Tarasov I.S., Fetisova N.V. *Pis'ma Zh. Tekh. Fiz.*, **26** (20), 40 (2000).
2. Golikova E.G., Kureshov V.A., Leshko A.Yu., Lyutetskiy A.V., Pikhtin N.A., Ryaboshtan Yu.A., Slipchenko S.O., Sokolova Z.N., Fetisova N.V., Bondarev A.D., Tarasov I.S. *Pis'ma Zh. Tekh. Fiz.*, **28** (3), 66 (2002).
3. Piprek J., White J.K., SpringThorpe A.J. *IEEE J. Quantum Electron.*, **38** (9), 1253 (2002).
4. Lyutetskiy A.V., Pikhtin N.A., Slipchenko S.O., Sokolova Z.N., Fetisova N.V., Leshko A.Yu., Shamakhov V.V., Andreev A.Yu., Golikova E.G., Ryaboshtan Yu.A., Tarasov I.S. *Fiz. Tekh. Poluprovodn.*, **37** (11), 115 (2003).

5. Lyutetskiy A.V., Borshchev K.S., Bondarev A.D., Nalet T.A., Pikhtin N.A., Slipchenko S.O., Fetisova N.V., Khomylev M.A., Marmalyuk A.A., Ryaboshtan Yu.A., Simakov V.A., Tarasov I.S. *Fiz. Tekh. Poluprovodn.*, **41** (7), 883 (2007).
6. Vinokurov D.A., Kapitonov V.A., Lyutetskiy A.V., Pikhtin N.A., Slipchenko S.O., Sokolova Z.N., Stankevich A.L., Khomylev M.A., Shamakhov V.V., Borshchev K.S., Arsent'ev I.N., Tarasov I.S. *Fiz. Tekh. Poluprovodn.*, **41** (8), 1003 (2007).
7. Lyutetskiy A.V., Borshchev K.S., Pikhtin N.A., Slipchenko S.O., Sokolova Z.N., Tarasov I.S. *Fiz. Tekh. Poluprovodn.*, **42** (1), 106 (2008).
8. Boucher J.F., Callahanb J.J. *Proc. SPIE Int. Soc. Opt. Eng.*, **8039**, 0390B-1 (2011).
9. Adachi S. *Properties of Semiconductor Alloys: Group-IV, III-V and II-VI Semiconductors* (Chichester: John Wiley & Sons, 2009).
10. Mircea A., Ougazzaden A., Primot G., Kazmierski C. *J. Cryst. Growth*, **124**, 737 (1992).
11. Veselov D.A., Pikhtin N.A., Lyutetskiy A.V., Slipchenko S.O., Sokolova Z.N., Shamakhov V.V., Shashkin I.S., Kapitonov V.A., Tarasov I.S. *Kvantovaya Elektron.*, **45** (7), 604 (2015) [*Quantum Electron.*, **45** (7), 604 (2015)].
12. Bert N.A., Bondarev A.D., Zolotarev V.V., Kirilenko D.A., Lubyanskii Ya.V., Lyutetskiy A.V., Slipchenko S.O., Petrunov A.N., Pikhtin N.A., Ayusheva K.R., Arsent'ev I.N., Tarasov I.S. *Fiz. Tekh. Poluprovodn.*, **49** (10), 1429 (2015).
13. Asryan L.V. *Kvantovaya Elektron.*, **35** (12), 1117 (2005) [*Quantum Electron.*, **35** (12), 1117 (2005)].
14. Gel'mont B.L., Sokolova Z.N. *Fiz. Tekh. Poluprovodn.*, **16** (9), 1670 (1982).
15. Gel'mont B.L., Sokolova Z.N., Yasievich I.N. *Fiz. Tekh. Poluprovodn.*, **16** (4), 592 (1982).